



**University of
Zurich** ^{UZH}

**Zurich Open Repository and
Archive**

University of Zurich
University Library
Strickhofstrasse 39
CH-8057 Zurich
www.zora.uzh.ch

Year: 2013

Red cell investigations: Art and artefacts

Minetti, Giampaolo ; Egée, Stephane ; Mörsdorf, Daniel ; Steffen, Patrick ; Makhro, Asya ; Achilli, Cesare ; Ciana, Annarita ; Wang, Jue ; Bouyer, Guillaume ; Bernhardt, Ingolf ; Wagner, Christian ; Thomas, Serge ; Bogdanova, Anna ; Kaestner, Lars

DOI: <https://doi.org/10.1016/j.blre.2013.02.002>

Posted at the Zurich Open Repository and Archive, University of Zurich

ZORA URL: <https://doi.org/10.5167/uzh-75686>

Journal Article

Accepted Version

Originally published at:

Minetti, Giampaolo; Egée, Stephane; Mörsdorf, Daniel; Steffen, Patrick; Makhro, Asya; Achilli, Cesare; Ciana, Annarita; Wang, Jue; Bouyer, Guillaume; Bernhardt, Ingolf; Wagner, Christian; Thomas, Serge; Bogdanova, Anna; Kaestner, Lars (2013). Red cell investigations: Art and artefacts. *Blood Reviews*, 27(2):91-101.

DOI: <https://doi.org/10.1016/j.blre.2013.02.002>

Red cell investigations: Art and artefacts

Giampaolo Minetti^{1,2}, Stephane Egeé^{1,3}, Daniel Mörsdorf^{1,4}, Patrick Steffen^{1,5}, Asya Makhro^{1,6}, Cesare Achilli^{1,2}, Annarita Ciana^{1,2}, Jue Wang^{1,7}, Guillaume Bouyer^{1,3}, Ingolf Bernhardt^{1,4}, Christian Wagner^{1,5}, Serge Thomas^{1,3}, Anna Bogdanova^{1,6}, Lars Kaestner^{1,7,*}

1 - *European Red Cell Society (www.)*

2 - *Department of Biology and Biotechnologies, Division of Biochemistry, University of Pavia, 27100 Pavia, Italy*

3 - *Station Biologique de Roscoff, UMR7150 Mer & Santé, 29680 Roscoff, France*

4 - *Biophysics Laboratory, Saarland University, Building A2 4, 66123 Saarbrücken, Germany*

5 - *Experimental Physics Department, Building E2 6, Saarland University, 66123 Saarbrücken, Germany*

6 - *Institute of Veterinary Physiology and the Zurich Center for Integrative Human Physiology (ZIHP), University of Zurich, Zurich Switzerland*

7 - *Institute for Molecular Cell Biology and Research Centre for Molecular Imaging and Screening, School of Medicine, Saarland University, Building 61, 66421 Homburg/Saar, Germany*

Abstract

Investigations of red blood cells include a wide range of methodologies ranging from population measurements with a billion cells evaluated simultaneously to single-cell approaches. All methods have a potential for pitfalls, and the comparison of data achieved by different technical approaches requires a consistent set of standards.

Here, we give an overview of the common methodological mistakes and how to avoid them. Additionally, we propose a number of standards that we believe will allow for data comparison between the different techniques and different labs. Here, we consider biochemical analysis, flux measurements, flow cytometry, patch-clamp measurements and dynamic fluorescence imaging as well as emerging single-cell techniques, such as the use of optical tweezers and atomic force microscopy.

1 Introduction

Contrary to a common belief, the red blood cell (RBC) is a cell type that is neither simple, nor easily obtainable in a pure form. Yet, it is probably the most studied cell type in the history of the life sciences starting with the microscopic observations of Jan Swammerdam in approximately 1660¹. Nevertheless, as in most other fields of science, contradictory data are common. Sometimes it is possible to unify initially opposing results, e.g., reconciling reports on the electrogenic permeabilities in malaria-infected RBCs^{2,3} or on the isolation of lipid rafts from RBCs⁴⁻⁶. In other cases, specific issues have not been completely resolved, for example, the number of Gardos channels per RBC^{7,8} or contradictory data regarding prostaglandin E₂-induced cation fluxes^{9,10,11}.

46 However, discrepancies often originate from different experimental protocols, inducing
47 different or even opposing degrees of artefacts. Sometimes, artefacts may lead to
48 completely wrong conclusions. This is a serious problem, as revealed in a recent
49 publication¹² in Nature. Here, a standard method intended for the isolation of
50 mononuclear cells (MNCs), based on the density-gradient centrifugation of blood, was
51 mistakenly used to isolate RBCs in an allegedly pure form. The entire paper is affected
52 by this artefact, but it obviously passed the review process in one of the most prestigious
53 journals.

54 To avoid this and other common artefacts, as well as to establish a basis for good
55 laboratory practices in RBC research, a subgroup of the European Red Cell Society
56 (ERCS) was formed to initiate standards for a better inter-methodological as well as
57 inter-laboratory comparison of RBC-derived data. As an initial attempt, here, we present
58 the first "guidelines" for avoiding artefacts in RBC research: In the first part, we discuss
59 the general challenges, such as obtaining pure RBC preparations, experimental
60 conditions in general and the comparison of studies between different species. In the
61 second part, we consider some of the most popular methods in RBC research,
62 discussing possible pitfalls, how to avoid them and the conditions for
63 comparing/combining different methodologies.

64 Our hope is that this report will be useful to those approaching the study of RBCs, to
65 avoid stumbling into major artefactual conditions and obtaining the best results from the
66 experiments.

67

68

69 **2 General considerations**

70

71 **2.1 Obtaining pure cell preparations**

72

73 The vast majority of biochemical studies, but also all other types of cell population
74 measurements, have been carried out, and still are, using bulk suspensions of
75 supposedly pure RBCs. The RBCs are obtained by sedimenting the cells by
76 centrifugation from a sample of whole blood that has been "washed" with variants of a
77 physiologic solution, followed by removal of the supernatant and the thin superficial layer
78 of cells. The latter, the so-called "buffy-coat", is indeed enriched in white blood cells
79 (WBCs), or leukocytes, but these cells belong chiefly to the MNC type, i.e., lymphocytes
80 and monocytes. The most abundant WBCs, however, the polymorphonuclear neutrophil
81 granulocytes (PMNs), tend to remain mixed with the RBCs owing to the similar density of
82 the two cell types, contaminating the RBC sample⁶. The only way of removing most of
83 the WBCs is by filtering the blood with leukodepletion filters. Roughly speaking, if the
84 total content of PMNs per million RBCs is 1000 in whole blood, it will decrease, at best,
85 to 100 in washed blood and to <10 in filtered blood⁶.

86 A simple and reliable procedure for RBC purification that is suitable for samples of small
87 volumes and easy to implement in every lab is filtration through cellulose, as was
88 originally proposed by Beutler et al.¹³ and described in detail in the supplementary
89 material of Achilli et al.¹⁴.

90 We propose this simple concept as a standard method and good laboratory practice in

91 RBC research. It should be emphasised, however, that filtration might not be applicable
92 in all instances, e.g., for pathological RBCs, because its functioning principle appears to
93 be based largely on the difference in deformability between RBCs and WBCs¹⁵. The
94 latter are much less deformable than normal RBCs and are therefore retained in the filter
95 for a longer time than RBCs. However, in certain RBC pathologies, RBC deformability is
96 abnormally reduced, and this may result in reduced filterability (hereditary spherocytosis,
97 hereditary elliptocytosis, ovalocytosis, sickle cell anaemia). The task of quantifying low
98 WBC levels is by no means a simple one, and special techniques have been devised for
99 this purpose. As a general remark, microscope counting using conventional
100 haemocytometer chambers is impractical and not sensitive enough. The flow cytometry
101 (FCM) approach is meaningful only if the number of total events counted in each
102 analysis is sufficiently high to reveal 1 WBC per 10⁶ RBCs, which implies long analysis
103 times¹⁶. An extremely sensitive and inexpensive method for the quantification of PMNs
104 in blood samples that can be easily implemented in all labs is the technique of gelatin
105 zymography, as recently adapted¹⁴.

106
107 *Typical artefacts*
108 The consequences of having a PMN-contaminated RBC suspension can be deleterious.
109 Two main types of artefacts can result from such a situation: (i) attribution to the RBCs
110 of a component/function that in fact belongs to the PMNs; (ii) damage to RBCs resulting
111 from hydrolases and oxidases released by activated or broken PMNs.

112 The first issue has already been exemplified in the introduction. As shown in Figure 1A,
113 the method results in the isolation of a fraction of RBCs together with all the PMNs that
114 were originally present in the blood sample, without even reducing the number of PMNs,
115 as would occur if a conventional centrifugation-based wash of the blood and removal of
116 the “buffy-coat” were performed.

117 The artefactual results that originate from PMN hydrolases damaging RBC components
118 are exemplified by the controversy on the isolation and characterisation of lipid rafts from
119 RBCs⁶. The most powerful and constitutively active hydrolases in the PMNs are the
120 serine proteases elastase and cathepsin G. These hydrolases are normally confined at
121 high concentrations in cytoplasmic vesicles (granules) and only released upon cell
122 activation. Detergents can easily free the proteases from the granules. It was shown that
123 even the presence of one PMN per million RBCs is able to release enough proteolytic
124 power to damage, if not fully inhibit, highly sensitive RBC proteins such as ankyrin and
125 protein 4.1⁶.

126 Another common situation that could give rise to artefactual results is the preparation of
127 “ghosts” from RBCs by hypotonic haemolysis. If the RBCs are contaminated by PMNs
128 and the buffers used are not effectively supplemented with anti-proteases, the RBC
129 membrane proteins will almost certainly be damaged (Figure 1B,C). The workaround to
130 this problem is the filtration of the blood and the use of freshly prepared lysing buffers
131 containing a working concentration of anti-proteases^{17,18}.

132 **2.2 Experimental conditions**

133
134
135 Other factors that must be standardised to be able to compare the obtained data

136 between different laboratories are the temperature, shear stress, medium content,
137 especially traces of serum, and the condition of cells used in the experiments.
138 Furthermore, recent studies emphasise the importance of co-factors and substrates of
139 several receptors, which may contribute to the experimental outcome. Those include the
140 presence of prostaglandins, hormones, amino acids and other natural or pathological
141 components of blood plasma.

142

143 *Possible artefacts and their causes*

144 (i) Temperature-related artefacts include ion misbalance and the following changes in
145 cell volume and Ca^{2+} -dependent processes. Temperature sensitivity depends on the
146 particular approach, but it can be severe, differing, e.g., between different types of ion
147 transporters. The decrease in the activity of ion transporters with a decrease in
148 temperature by 10 degrees (Q10) is approximately 30-fold for the Ca^{2+} -ATPase¹⁹,
149 approximately 3-fold for the Na^+/K^+ -ATPase²⁰ and approximately 1.5-3-fold for most of
150 the ion transporter systems^{21,22}. Thus, temperature changes may have a pronounced
151 effect on the intracellular Ca^{2+} levels and the Na^+/K^+ distribution. The temperature may
152 not be fixed at 37°C in particular experimental settings (e.g., controlling the
153 temperature can be complicated for patch-clamp investigations). However,
154 temperature as a factor has to be taken into account, and the potential side effects
155 must be controlled.

156 (i) Serum and the multiple biologically active factors it contains, including albumin and
157 factors bound to it, such as interleukins, prostaglandins, insulin and amino acids, can
158 introduce artefacts. Depending on the experimental settings, investigations are
159 conducted in serum-containing or serum-free media. Proteins introduced with serum
160 have been shown to play an active role in regulating the activity of ion transporters in
161 RBCs obtained from healthy and diseased subjects. Little is known about the serum
162 components mediating the effects. It has been shown that PGE_2 activates Ca^{2+} uptake
163 by RBCs^{10,23}. Insulin interacts with its receptors, inducing activation of eNOS in
164 RBCs²⁴. From studies on malaria-infected cells, it is now well recognised that traces
165 of serum change the membrane conductance upon infection^{2,25}. Nevertheless, such a
166 phenomenon may also be observed when performing experiments on uninfected
167 cells²⁶. This leads to the conclusion that serum-proteins play a role in modulating the
168 activity of transport proteins²⁷. This is a potential source of discrepancy between
169 single cell and bulk measurements. In most of the latter, at least serum albumin is
170 present (usually 5%) as a supplement in the suspending medium. The presence of
171 several amino acids in the incubation medium makes a substantial difference in the
172 response of cells to oxygen, insulin and erythropoietin stimulation. Among these
173 amino acids are L-arginine, which is a substrate for endothelial nitric oxide synthase¹⁸,
174 and the N-methyl D-aspartate receptor agonists glutamate and glycine, as well as
175 homocysteine, which stimulates Ca^{2+} uptake by human and rat RBCs²⁸. Treatment of
176 RBCs with relatively high concentrations of orthovanadate in the presence of 1-2 mM
177 extracellular Ca^{2+} results in irreversible pathological alterations of cell morphology,
178 followed by blebbing and finally the loss of membrane integrity, particularly at room
179 temperature when the Ca^{2+} pump function is reduced (Figure 2A). This often remains
180 unnoticed when working with RBC suspensions.

181 (ii) Intercellular differences originating from storage (fresh cells vs. stored cells and
182 storage conditions), inter-individual and inter-cellular variability are sources of
183 artefacts. Often, stored/conserved RBCs are used for measurements. RBC
184 preservation media are Ca^{2+} -free, low in Na^+ and enriched with K^+ and glucose. RBC
185 preservation results in gradual adenosine triphosphate (ATP) and 2,3-
186 bisphosphoglycerate deprivation and oxidation of glutathione, which begin after one
187 day of storage (Figure 2B). Replacement of the storage medium with Ca^{2+} -containing
188 plasma-like medium (1.8 mM CaCl_2 , 150 mM NaCl , 4 mM KCl , 5 mM glucose) results
189 in the events illustrated in Figure 2B. The cells will shrink due to acute Ca^{2+} overload,
190 and further ATP deprivation occurs due to acute activation of the Na^+/K^+ -ATPase and
191 Ca^{2+} -ATPase caused by acute Na^+ and Ca^{2+} overload. The results obtained using such
192 cells may hardly be compared with those obtained from fresh RBCs. Restitution of
193 stored cells may be useful for avoiding storage-induced artefacts. Preconditioning of
194 stored blood (rejuvenation) has been proposed²⁹, and the corresponding
195 "Rejuvenation Solution" (Rejuvesol; enCyte Systems, Inc., Braintree, Mass)
196 containing phosphate, inosine, pyruvate, and adenine, or 15 mM D-ribose was shown
197 to be beneficial when applied before the transfusion³⁰. Because the components of
198 rejuvenation solutions actively interfere with intracellular metabolism and the redox
199 state, we propose to use a "minimally invasive" preconditioning protocol. The stored
200 cells are re-suspended in the incubation medium of interest in the presence 0.5 mM
201 Ca^{2+} , 10 mM glucose and 0.1% BSA at room temperature one hour prior to the
202 experiment. This time is required to restore the activity of the Ca^{2+} pump at a sub-
203 physiological temperature and to provide substrates for glycolytic enzymes.

204 Most artefacts arise from the lack of attention to these factors. The composition of
205 incubation media varies markedly between experiments. The impact of oxidation,
206 methaemoglobinemia, phosphatidyl serine (PS) exposure and other membrane-related
207 events, as well as that of the addition of ion transport inhibitors (e.g., vanadate often
208 present during Ca^{2+} uptake measurements, see Figure 2A), on the cell morphology, ion
209 content, redox state and metabolic status may be dramatic, but it has rarely been taken
210 into account.

211 The redox status of the cells is an important parameter to control. Oxidation has a
212 profound effect on metabolism, regulation of cell volume, and cytoskeletal structure.
213 Reducing cell deformability induces Ca^{2+} entry, leading to PS exposure, membrane
214 blebbing and eventually premature cell death³¹. Nevertheless, it was also shown that
215 oxidation may activate anion channels, mimicking pathways that are activated upon
216 malaria infection^{32,33}. Even if the threshold seems to be rather high, the oxidation level
217 might be high enough in some cells to trigger artificial responses in some protocols.
218 Most importantly, throughout their lifetime, RBCs are continuously exposed to high
219 oxidative stress. Oxidative defence capacities may decrease with RBC aging³⁴, and
220 senescent RBCs show alterations (e.g., increased denaturation of haemoglobin,
221 membrane binding of hemichromes and free iron, aggregation of band 3 protein,
222 deposition of antibodies and complement fragments, PS exposure) similar to those of
223 oxidised cells^{35,36}.

224 Facilitated ageing occurring under conditions of sheer stress (e.g., in patients with
225 polycythaemia) is also associated with oxidative stress³⁷. Furthermore, storage of RBCs

226 results in progressive oxidative stress and loss of reduced glutathione along with ATP
227 deprivation. For that reason experimental observations obtained using RBCs from a
228 blood bank may differ significantly from those generated using freshly withdrawn blood.
229 Further support comes from whole-cell patch-clamp experiments reporting that oxidation
230 induced anion selective currents^{32,38,39}.

231 Sufficient levels of glucose, a lack of Ca²⁺ overload and sheer stress are essential for
232 maintenance of the citrate-containing glutathione pool. Recent studies revealed that
233 some plasma components are required for endothelial NO synthase to function. L-
234 arginine (100-300 μ M) and nitrite (~150 nM in human plasma) are essential for
235 maintenance of NO production by RBCs under normoxic and hypoxic conditions,
236 respectively^{24,40}, and their absence in the incubation medium, as well as manipulation of
237 the intracellular Ca²⁺ levels, will result in uncoupling of NO production and progressive
238 oxidative stress, especially when the treatment includes manipulation of oxygen levels or
239 activation of NO synthase^{18,28,41}.

240 Another example of the importance of the ionic composition of the incubation media
241 arises from patch-clamp measurements of malaria-infected RBCs: Whereas at
242 physiological saline concentrations, at least two different types of anion channel activity
243 can be described, when supraphysiological concentrations of Cl⁻ are used^{42,43}, one of the
244 channels has (i) a saturated single conductance and (ii) an open probability close to zero
245 above the threshold chloride concentration³. This last phenomenon explains the majority
246 of the discrepancies reported in the field, and it is tempting to think that the same
247 limitation may apply to uninfected RBCs.

248

249 **2.3 Interspecies studies**

250

251 The challenge of how to compare studies performed in different species is widespread in
252 biomedical science. The power of genetic manipulation in combination with the short
253 generation cycle makes mice an increasingly popular animal model. Obvious
254 advantages often overwhelm concerns about the reliability of results derived from animal
255 models of human diseases. This problem also applies to RBC research and originates
256 from the fact that the basic characterisation of mouse RBCs is rather limited. Before the
257 advent of transgenic animals, mice were not a particularly widespread model for
258 studying RBCs.

259

260 *Potentials of comparative studies*

261 Comparative RBC research continues to build on species-specific studies involving, e.g.,
262 domestic animals. In this field, a substantial number of publications and even textbooks
263 are available^{44,45}. Sometimes, the switch to animal RBCs may provide invaluable
264 advantages over human RBCs. These advantages might be such simple properties as
265 the cell size. For instance the amphiuma RBCs have an elliptical size of ~62 μ m in
266 length and ~36 μ m in width and are used to perform the initial potential measurements in
267 RBCs⁴⁶. The RBCs of fish (6.5-44.6 μ m diameter), amphibians (16-70 μ m) and birds
268 (9.7-15.4 μ m) contain organelles such as a nucleus, mitochondria and ribosomes. These
269 qualitative differences compared to human RBCs might be advantageous or
270 disadvantageous and can be used as experimental tools.

271 The great variations in RBCs between species on the one hand and a broad
272 conservation on the other hand allows the use of animal RBCs as particular models for
273 certain protein manipulations, even in the organelle-free mammalian RBCs, that would
274 otherwise require the breeding of transgenic animals. Examples include the RBCs of
275 carnivora that lack the Na⁺/K⁺- pump⁴⁷ (instead, they have a Na⁺/Ca²⁺ exchanger, which is
276 absent in the RBCs of other species) or sheep RBCs that do not seem to contain
277 scramblase⁴⁸. There is list of differences⁴⁹ that cannot be covered in this paper –
278 furthermore, the protein and lipid distributions of RBCs between species can differ
279 considerably^{50,51}.

280 Thus, vast amounts of information on the alternative models that may be used to study
281 the pathological alterations in human RBCs are not used. Making the results of
282 comparative studies on RBCs more “visible” will help to acknowledge the advantages
283 that these cells provide.

284 Knowing all these differences, it should be a habit of good laboratory praxis (as well as
285 reviewing praxis) to either perform studies (publications) just within a defined species or,
286 when mixing species, to show - whenever possible - explicitly the transferability of the
287 "previous step", at least in the supplemental material. This rule of course needs to be
288 adapted if the animal model is used as a "modified source" of RBCs.

289
290

291 **3 Methodological considerations**

292

293 **3.1 Proteomics**

294

295 Proteomics is most likely the method that is most affected by contamination of cell
296 preparations, as outlined in 2.1, Obtaining pure cell preparations. This holds true
297 because proteomic studies are still carried out on cell suspensions, although single-cell
298 approaches have been introduced⁵².

299 The importance of the pure cell preparations is efficiently and impressively illustrated by
300 some of the most recent proteomic studies, where care was taken to reduce WBC
301 contamination of the RBCs, resulting in a list of less than 300 recognised RBC
302 membrane proteins⁵³, compared to the much larger number of supposedly erythrocytic
303 proteins presented in earlier catalogues.

304 Presently, the proteomic studies of RBCs are still somewhat separated from functional
305 studies, resulting in protein catalogues that do not (yet) fit with functional identified
306 proteins from, e.g., patch-clamp recordings. Bridging this gap will be one of the
307 challenges of future RBC research.

308

309 **3.2 Ion fluxes**

310

311 Measurements of ion fluxes through the RBC membrane are performed using various
312 approaches. Radioactive tracers have been used for unidirectional flux measurements
313 for many decades. This technique allows quantification of unidirectional movements of
314 ions by electroneutral and electrogenic ion transporters as well as residual ion fluxes.
315 Other methods to assess ion movements through the membrane are based on

316 monitoring of net ion uptake/loss by means of ion-selective electrodes, flame photometry,
317 atomic absorption spectrophotometry, etc.

318 Accumulation or loss of radioactive tracers may be estimated with high sensitivity (up to
319 single disintegration events) using beta- and gamma-counters. For most ions, the
320 corresponding radionuclides, which may play a role as isotopic carriers, have relatively
321 long half-lives (weeks to months). Rubidium-86 ($T_{1/2}=18.6$ d) is often used as a tracer
322 because the most suitable $^{42}\text{K}^+$ radionuclide has a rather short half-life ($T_{1/2}=12.5$ h) and
323 requires a supply for fresh radioisotopes, e.g., the proximity of a cyclotron to the lab
324 where the ion fluxes are assessed. With some rare exceptions⁵⁴, discrimination between
325 K^+ and Rb^+ by ion transport systems in RBCs does not exceed 20%⁵⁵.

326
327 *Pitfalls and limitations*
328 For monitoring the kinetics of the radioactive tracer distribution, one may assess the
329 unidirectional inward and outward fluxes as well as a steady-state distribution of
330 selected ion species between the cell and the medium, considering that the cell lacks
331 compartmentalisation. If this is not the case, as for intracellular Ca^{2+} , in RBCs of patients
332 with sickle cell disease⁵⁶, cytosolic free Ca^{2+} cannot be estimated from the $^{45}\text{Ca}^{2+}$
333 distribution between the cells and the medium. Most of the Ca^{2+} in that case is
334 accumulated in the intracellular inside-out vesicles that are most likely enriched with Ca^{2+}
335 pumps⁵⁷, and an increase in the intracellular $^{45}\text{Ca}^{2+}$ levels is not always followed by the
336 activation of Ca^{2+} -sensitive K^+ (Gardos) channels.

337 All discussed, measurements of ion fluxes bear a common limitation: flux measurements
338 are performed in suspension, and the considerations discussed in 2.1, Obtaining pure
339 cell preparations, apply. So far, studies to assess the role of WBC and platelet
340 contamination in possible artefact generation when measuring ion fluxes using
341 radioactive tracers are lacking.

342 Another point that is seldom taken into account is the effect of the electro-neutrality of
343 compartments on ion movements. Cation movements, such as those mediated by
344 Gardos channel activity, that lead to cell dehydration are known to be rate limited by
345 anion movements. In many cell suspension experiments, thiocyanate (SCN^-) is used to
346 bypass this limitation of anion movements. Ten millimolar is usually sufficient to saturate
347 this effect⁵⁸, avoiding important changes in the isoelectric point of impermeant anions
348 and RBC hydration that are observed at higher SCN^- concentrations⁵⁹. Apart from ion
349 flux experiments, this could also apply to patch-clamp experiments aiming to investigate
350 cation channel activity. Even if this consideration does not apply in the whole-cell
351 configuration because the anion supply is provided by the pipette content, it can impair
352 the movement of cations in the cell-attached configuration. In this case, run-down of
353 channel activity might be observed and conclusions can be drawn erroneously.

354 355 **3.3 Patch-clamp**

356
357 During the past three decades, electrophysiological studies have revealed that the
358 human RBC membrane is endowed with a large variety of ion channels⁶⁰⁻⁶⁴. However,
359 their physiological role remains widely unclear; they barely participate in the RBC
360 homeostasis, which is based on an almost total absence of cationic permeability and

361 minute anionic conductance⁶⁵. Nevertheless, due to the pioneering work of Hamill on
362 human and frog RBCs^{58,66}, the patch-clamp technique applied to RBCs has proven to be
363 a powerful method to decipher the involvement of ionic conductances mainly in
364 pathophysiological scenarios^{32,42,59,62,67-69}.

365

366 *Challenges to patch-clamp RBCs*

367 The main problem when attempting to perform patch-clamp on RBCs lies in the small
368 size of the cells, which especially holds true for mammalian RBCs (2.1-9.4 μm) (cp. 2.3,
369 Interspecies studies). This small size imposes four major challenges:

370 (i) The opto-mechanical properties of the hardware require high-quality microscopes and
371 at least 20x objectives. A 40x objective with phase or Nomarski contrast is usually
372 necessary for recordings on malaria-infected cells to recognise the infected RBCs.
373 When approaching the pipette to form a seal, very precise micromanipulators are
374 required.

375 (ii) RBCs are “designed” for passing through small capillaries. When passing through the
376 spleen, RBCs have to go through tiny slits whose mean size has been recently
377 measured at 1.89 μm in length and 0.65 μm in width⁴³. Therefore, patch-pipette tips
378 must be rather thin, with an opening smaller than 1 μm (corresponds to roughly 10-15
379 M Ω in physiological saline solutions) to avoid the entry of the cell into the pipette.
380 Besides the pipette size, its shape has to be adapted such that a piece of membrane
381 enters the pipette for seal formation without totally entering into the pipette when
382 depression (typically 20 mbar) is applied. The pipette tip must be thin enough, but at
383 the same time tapered enough, to preserve a low R_{access} value (see (iii), below). Another
384 issue arises from RBC’s high deformability. The portion of the RBC membrane that
385 enters into the pipettes during seal formation varies. Furthermore, it has been
386 recognised that membrane deformation induces transient Ca^{2+} entry in RBCs⁷⁰. Such
387 transient activity may generate secondary transient anionic channel activity⁷¹. This
388 phenomenon leads to a change in the intracellular K^+ concentration that has to be
389 taken into account for data interpretation. Therefore, the time of seal formation and
390 calibrated depression must be mentioned in publications.

391 (iii) Electrical issues have to be considered, notably for the whole-cell configuration.
392 Figure 3 describes the electric model for the cell-attached configuration and the
393 whole-cell configuration. Do the limitations described in Figure 3 apply to RBCs?
394 From suspension experiments, the membrane resistance R_m of human RBCs was
395 estimated to be in the range of $10^6 \Omega\text{cm}^2$, with chloride resistance R_{Cl} ranging between
396 10^5 and $10^6 \Omega\text{cm}^2$ ⁷². Given a mean surface of 135 μm^2 , the whole-cell resistance can
397 be estimated to be between 10 and 40 G Ω . This is in the range of the seal values of
398 patched RBCs and explains why whole-cell experiments were not used on RBCs for a
399 long time⁷³. The conductance was estimated to be too low to discriminate properly
400 between channel activity and seal leakage. However, the membrane resistance can
401 be considerably lower when the ion channels in the RBC membrane are activated.
402 Anion conductance rises to several nS, e.g., in PKA-activated, oxidised or malaria-
403 infected RBCs, and cation conductance can be triggered when cation channels are
404 activated. Thus for whole cell experiments, R_m remains much lower than R_{seal} , and the
405 current and voltage do not suffer high distortion. Another parameter to take into

406 account is the pipette access resistance R_{access} . Because the pipette tip must be rather
407 narrow when patching RBCs, precautions must be taken. The R_{access} value is
408 determined by the pipette geometry, solution composition and possibly by the
409 presence of cell debris generated by membrane rupture. The use of pipettes
410 immediately after pulling, their adapted shape, with rapidly tapering geometry, and the
411 filtering of all pipette solutions with $0.2 \mu\text{m}$ filters helps to maintain low R_{access} values.
412 (iv) The small RBC size results in a small membrane capacitance of approximately 1-
413 $1.3 \text{ pF}^{74,75}$. This becomes relevant during the transition from the cell-attached to
414 whole-cell configuration. The rupture of the membrane fragment inside the pipette tip
415 is typically achieved by a brief electrical pulse (200 ms, 500 mV). A successful whole-
416 cell configuration can be checked via the sudden appearance of membrane
417 capacitance transient currents, which can be easily compensated on the amplifier.
418 Nevertheless, the situation is different in plate-based “pipettes” as they are used by
419 automated patch-robots (cp. Figure 4). There, the basal capacitance of the plate is
420 much higher and an increase of 1 pF is almost invisible. Therefore, the major
421 indication for reaching the whole-cell state is the increase in current, which is a
422 challenge because differentiation between the loss of seal resistance and the whole
423 cell current needs to be probed in the experimental protocol. However, if the seal
424 resistance is approximately $10 \text{ G}\Omega$, the current leakage at +100 mV can be calculated
425 to be 10 pA, presenting a relation to Ohm’s law. Typical whole-cell recordings show
426 current values between 200 to 1000 pA or even higher, which often are rectifying, i.e.,
427 they do not follow Ohm’s law; then, the leak always remains below 1-5% of the total
428 current.

429 The automated patch-clamp recordings were used to test for the heterogeneity of naive
430 RBC conductance among the RBCs of a donor as well as investigating the variability
431 between different donors. Figure 4 depicts such a comparison for 2 healthy donors.
432 The simultaneous measurements of 4 to 96 RBCs (depending on the model of the
433 automated patch systems) allow for measurement of a population of RBCs with exactly
434 the same experimental procedure, and there is no experimental bias towards choosing a
435 (particular) cell. In contrast, classical patch-clamp allows for more (visual) control over
436 the particular experiment/cell and at least an order of magnitude lower noise level,
437 typically approximately 1 pA.

438 *Comparison of Patch-clamp data with other entities*

439 Comparing data from cell suspension experiments (cp. 3.2, Ion fluxes) and those issued
440 from patch-clamp studies is a common but difficult task, which can be exemplified by the
441 entry of Ca^{2+} observed in sickle cells upon deoxygenation. This entry, designated P_{sickle} , is
442 best characterised as a poorly selective permeability pathway for small, inorganic
443 monovalent and divalent cations⁷⁶. Experiments in which the fraction of activated cells
444 was studied as a function of the external Ca^{2+} concentration showed that sickling is a
445 stochastic event of random intensity among HbSS RBCs, capable of generating maximal
446 Gardos channel activation in a small fraction of cells during each deoxygenation-sickling
447 pulse. Consistent with the stochastic nature of P_{sickle} , repeated pulses led to the
448 progressive accumulation of dense cells, whereas a single long pulse caused only an
449 early production of a single small fraction of dense RBCs⁷⁷. Lew *et al.* eventually
450

451 depicted this nature clearly by writing: “When electrophysiologists finally approach the
452 study of P_{sickle} under patch-clamp, they ought to bear in mind the probabilistic nature of
453 P_{sickle} in each deoxygenation pulse before consulting their psychiatrist for the lack of
454 reproducibility!”⁷⁶

455 One has to keep in mind that electrophysiology conclusions are drawn from results
456 where the membrane potential is changed at will by the experimenter, meaning that they
457 are rarely obtained at the resting membrane potential, rendering comparison with cell
458 suspensions difficult. This is exemplified in a recent study, where it was shown that
459 increased membrane permeability for sorbitol in malaria-infected RBCs could not easily
460 be reconciled with data from whole-cell experiments⁷⁸. Indeed, in isosmotic sorbitol
461 haemolysis, the membrane potential reaches values above +50 mV due to the absence
462 of charges at the extracellular side of the membrane. Subsequent comparison of these
463 data to that obtained with patch-clamp (at this membrane potential, inwardly rectified
464 currents induced by infection are almost totally abolished^{59,62}) seems impossible.

465

466 **3.4 Flow cytometry**

467

468 FCM is a technique that uses optical detection methods for counting and analysing
469 particles in the size range of micrometres. In comparison to microscopic investigations of
470 single RBCs (see below), the application of FCM and cell sorting present some
471 advantages as well as disadvantages.

472

473 *Advantages*

474 A major advantage of FCM compared to single-cell imaging is the inherent analysis of a
475 larger amount of cells within a shorter time (a minimum of several 10,000 cells vs. a few
476 hundred cells). This reduces the statistical noise. The gating for cell populations is easy
477 and reduces the analysed cells to a dedicated population out of a heterogeneous sample.
478 The forward scatter mode shows the size distribution of the cells. Although it is by no
479 means an exact measure of the absolute cell volume, it can be used as an indicator of
480 the relative size changes of the RBC samples.

481 The side scatter mode shows the “granularity” of the cell, which is related to the
482 complexity of structures in the cell interior. It can provide information on the presence of
483 different cell types in a single suspension of cells (e.g., in blood). A useful feature of flow
484 cytometry is connected with the possibility of measuring the fluorescence emitted by
485 suitable fluorochromes that are used as probes for a given particular cell property.
486 Fluorescently labelled antibodies and fluorescent probes sensitive for a particular
487 chemico-physical parameter of the cell (e.g., pH, Ca^{2+} , PS exposure, mesomorphic state
488 of the lipids) are the most commonly used fluorescent molecules.

489

490 *Limitations*

491 Due to the measurement technique, cells have to pass the cuvette in a high-speed fluid
492 stream. This limits measurements to cells in a suspension and excludes larger
493 aggregates. However, doublets of RBCs can be easily recognised by the fluorescence
494 signal forward or side scatter. Although the side scatter is an indicator for the granularity
495 and surface shape, it is not possible to measure and reliably distinguish the different

496 shapes (echinocytes, discocytes, stomatocytes) of RBCs. In the forward and the side
497 scatter, RBCs present shapes that are nearly similar and overlapping signals.

498 The fluorescence intensities observed by FCM are integrated values of the entire cell
499 and do not resolve a subcellular distribution of the fluorescence as in imaging (see
500 below).

501 In some experiments, the formation of microvesicles can be observed. Due to the small
502 size of the microvesicles, they will be shown in the forward and side scatter below the
503 threshold together with the cell debris and dead cells and will normally be discarded.
504 However, the fluorescence might be used to discriminate the vesicles from the debris,
505 and this could allow a quantitative analysis.

506 In contrast to single-cell imaging approaches, it is not possible to follow the kinetics of
507 any signal in a single cell. After measurement of the optical parameters, the cell is either
508 discarded or collected in a tube with RBCs depicting the same properties.

509 In all fluorescence measurements of RBCs, haemoglobin shows a strong absorption of
510 UV and visible light (for more details and discussion, see 3.5, Cellular Imaging). This
511 requires dyes with emission wavelengths above 600 nm or brighter fluorophores
512 (compared to thresholds that are known for haemoglobin-free cells).

513

514 *Potential artefacts*

515 Before measuring the different parameters, the cells are sucked under pressure in a fluid
516 stream through a small capillary into the measurement chamber. While the cell
517 suspension is passing through a capillary in the FCM to the measurement chamber, the
518 cells can be exposed to shear stress because of the different speeds of the sample and
519 the sheath fluid. An applied shear stress can induce different mechanisms such as the
520 activation or inactivation of physiological processes in the cells (e.g., Ca^{2+} increase in
521 RBCs exposed to mechanical stress⁷⁹) or even damage the membrane. Values for the
522 applied pressure can reach 500 kPa and higher (manufacturer information), which
523 exceed the normal systolic arterial blood pressure value of approximately 15 kPa by a
524 factor of more than 30. It is well known from other cell types that cell damage can occur
525 because of the applied pressure⁸⁰, and our own observations showed that a population
526 of fragile RBCs (observed in imaging) can disappear in FCM (unpublished observations).

527

528 **3.5 Cellular Imaging**

529

530 Live cell imaging is a popular method to explore cellular signalling⁸¹. However, for the
531 investigation of RBCs, it is rather sparsely applied. This might be due to three major
532 drawbacks:

533 (i) The absorption spectrum of the haemoglobin heavily interferes with the absorption of
534 many commonly used dyes and additionally quenches their emission, as exemplified
535 by the most popular Ca^{2+} fluorophores (Figure 5).

536 (ii) Due to the lack of a protein translation mechanism, the application of fluorescent
537 proteins and genetically encoded biosensors as an emerging tool in biomedical
538 research is limited to the generation of transgenic animals (cp. also ⁸²).

539 (iii) In live cell imaging (time laps), each experiment follows a substantial number of
540 cells (not just one as, e.g., in patch-clamp recordings), and each cell is followed over

541 an arbitrary time course (not just one time point as, e.g., in FCM). This leads to a
542 large amount of data. In light of the increasing awareness that RBCs can form a
543 highly heterogeneous population (cp. Figure 4), there is a requirement for analysis
544 guidelines that are not yet filed and that would exceed the size of this section.
545 Although these 3 points are serious and have to be taken into account, cellular imaging
546 is a powerful tool in RBC research.

547 *Potential artefacts and how to avoid them*

548 A number of points have to be considered to avoid artefacts. In imaging approaches,
549 dye molecules and photons are used to probe the cells. Photons can interact with the
550 cellular constituents and may induce what is commonly referred to as phototoxicity. For
551 RBCs, this is known for near infrared light⁸³ and for the interaction of UV light with
552 haemoglobin, resulting in the generation of a highly fluorescent photoproduct, most likely
553 bilirubin⁸⁴.

554 The interaction of the photons with the dye can lead to photobleaching and induce a
555 "loss of signal". This decreased fluorescence leads to underestimation of the signal of
556 interest. Furthermore, there is another almost opposite effect that is often neglected but
557 may occur with some dyes, e.g., with Fluo-4, the so-called "antibleaching". This is, in this
558 example, the light-mediated induction of Ca²⁺ insensitive but highly fluorescent dye
559 molecules that can occur if illumination of high intensity is used. Consequently, the
560 signal of interest is prone to be overestimated.

561 Additionally, triple interactions between endogenous proteins, fluorescent dyes and
562 photons may alter the properties of the fluorescent read-out. If there is a binding affinity
563 between the endogenous proteins and the fluorescent dye under certain conditions⁸⁵,
564 Förster Resonance Energy Transfer (FRET) occurs and consecutively alters the
565 fluorescence intensity, spectral properties and fluorescence lifetime. In RBCs, FRET can
566 occur, e.g., between the dye Fura-red and haemoglobin (unpublished results).

567 It must be noted that FRET can also be used in a beneficial way, as nicely shown by
568 Esposito et al.⁸⁶ for imaging the haemoglobin concentrations in malaria-infected RBCs.

569 Yet another factor that influences the fluorescence intensity is RBC volume changes
570 because a change in volume results in a change in the dye concentration and hence an
571 altered fluorescence signal.

572 Fortunately, most of the above mentioned sources of artefacts are rather small and
573 might be neglected when the observed signals are robust. However, if minute signals
574 are expected or observed, the artefacts are likely to become relevant.

575 An almost unavoidable artificial situation in live cell imaging is the fact that the RBCs are
576 attached to a (coated or uncoated) coverslip. The only way to exclude artificial
577 conclusions is the comparison/combination with complementary methods.

578 Last but not least, live cell imaging is often used to detect hormonal or pharmacological
579 stimulation of RBCs. To have a proper control of the solution surrounding the cell, a local
580 perfusion (a micro-manipulator-associated cannula placed close to the RBCs to apply a
581 laminar flow) is preferred over an exchange of the bulk solution of the entire dish that
582 almost certainly would lead to slow gradients of the exchanged solutions and a loss of
583 control concerning the timing of the drug or hormonal stimulation. Because RBCs
584 contain a number of mechanically sensitive proteins³⁸, one has to make sure that the
585

586 flow does not change with the application, and therefore, the flow must be kept constant
587 (also under control conditions) and just the solution composition needs to be switched
588 from the battery of solutions.

589

590 **3.6. Adhesion force measurements**

591

592 Adhesion is traditionally measured by either microscopic investigation, quantifying a
593 microscopic aggregation index⁸⁷ or by indirect methods based on the properties of RBC
594 suspensions. Such techniques include sedimentation-associated procedures,
595 transmission light or ultrasound scattering, impedance measurements, determination of
596 viscosity or other rheometric methods⁸⁸. The classical methods to measure RBC
597 aggregation have been recently reviewed⁸⁹. However, with regard to adhesion force
598 measurements, rheometric techniques have widely been used^{90,91}. These methods are
599 all indirect and suffer from a limited amount of information on the number of cells
600 involved or the impact of RBC morphological and deformability changes.

601

602 *Quantitative force measurements*

603 Recently, two quantitative RBC intercellular adhesion measurements were introduced at
604 the single-cell level and compared to each other^{92,93}. The two techniques are
605 holographic optical tweezers (HOT) and atomic force microscope-based single cell force
606 spectroscopy (SCFS). To exert forces on cells with optical tweezers, a limited force
607 regime is available due to cell damage with increasing laser power, i.e., there exists an
608 upper limit of force at which the adhesion forces between cells can be measured. In
609 addition to that, a lower limit of measurable adhesion forces exists for the SCFS, which
610 is due to both the limited force resolution of the system and the squeezing of the cells
611 during the measurements that can possibly induce adhesion force artefacts (see below).
612 Both limits could be illustrated by measuring the small adhesion forces between single
613 RBCs under physiological conditions^{92,93}. In the course of the experiment, a cantilever
614 with an attached cell was lowered onto another cell that was attached to the substrate
615 until a preset defined constant force was reached and kept stationary for a defined
616 contact time (Figure 6A). Subsequently, the cantilever was withdrawn at a constant
617 speed. During the approach and retraction, the cantilever was deflected as a
618 consequence of the acting forces. This deflection, which is proportional to the acting
619 forces, was recorded in force-distance curves (Figure 6C). The retraction curve was
620 typically characterised by the maximum force required to separate the cells from each
621 other, referred to as the maximum unbinding force. Under physiological conditions,
622 RBCs should not adhere at all. Hence, it was expected that a very small force close to
623 zero would be achieved. In contrast, a mean force of approximately 29 pN was
624 measured. To determine if this force was real or an artefact of the SCFS technique itself,
625 HOT measurements were conducted. The HOT exerts a force of 15-20 pN (Figure 6D)
626 at most because a higher laser power would damage the RBC.

627 Considering the mean adhesion forces of 29 pN derived under control conditions from
628 the SCFS measurements, it should not be possible to separate two RBCs by the use of
629 HOT once they have touched each other. Surprisingly, in the measurements with the
630 optical tweezers, it was possible to easily separate the cells. Even more surprisingly, it

631 was difficult to detect any adhesion force at all (Figure 6D).
632 The only way to explain the difference in both techniques is the slightly invasive nature
633 of the SCFS. An inevitable part of the SCFS measurements is the requirement for a
634 preset force set point that is used as a marker if both cells have come into close contact
635 (i.e., squeezing the two cells together with a certain set point force). This invasive
636 squeezing of the cells is artificial, and it most likely induces a small adhesion by itself.
637 The above mentioned problems should not arise when probing RBCs for specific
638 molecules, e.g., for testing receptor binding⁹⁴. In this case, the cantilever is
639 functionalised with the specific molecules (e.g., fibrinogen) and allows measuring the
640 adhesion between a molecule-coated cantilever and the RBC.

641
642 *Selection criteria for force measurements*
643 When measuring forces between RBCs, it would be desirable to combine the
644 complementary methods of SCFS and HOT. Unfortunately, both methods are complex
645 and laborious, and this advice might not always be feasible. Therefore, the tool can be
646 chosen according to the dimension of the expected force. The SCFS is advised for
647 adhesion forces larger than 30 pN and the HOT for adhesion forces smaller than 30 pN.
648 While the squeezing of the cells in the SCFS measurements is the critical parameter, the
649 laser power is the critical parameter in the HOT measurements.

650
651

652 **4 Conclusions**

653
654 We are left with the impression that a significant portion of the past literature on RBCs
655 should be re-read to verify whether it could have been affected by the problem of cell
656 contamination. Of course, one will not incur such problems when studying RBCs at a
657 single-cell level.

658 Recent studies reveal that RBC populations are rather heterogenous¹⁰, as depicted in
659 Figure 4, which may result in additional problems when working with bulk suspensions
660 as well as with single RBCs. A major reason for the inhomogeneities of circulating RBCs
661 are differences in the cell age⁹⁵. There are indications that the plasma membrane Ca²⁺
662 pump activity decreases with RBC age in a monotonic fashion, which may lead, at least
663 for some cells, to changes in the sodium and potassium content. However, when
664 performing single-cell experiments, the cells are chosen randomly, i.e., cells can be from
665 one or the other end of the age scale. Moreover, variable amounts of circulating
666 reticulocytes also contribute to the variability of measurements performed on bulk RBC
667 suspensions, even after WBCs and platelets have been carefully removed. Therefore, a
668 flow chart of an optimised protocol for studying a property/component of mature RBCs
669 should involve the following: leukodepletion by any suitable method/filter; gelatin
670 zymography to ascertain the level of residual PMNs; the efficient use of anti-proteases;
671 reticulocyte quantification (count and/or Western Blotting of, for instance, CD71, the
672 transferrin receptor); separation of RBCs into subpopulations of different density/age
673 and isolation of a population of “mature” RBCs⁹⁵. However, the availability of a reliable
674 and artefact-free separation technique is still debated.

675 Alternatively, to elucidate the inter-cellular variability of responses, measurements in cell

676 suspensions should be combined with single-cell techniques such as fluorescent live cell
677 imaging, FCM and/or patch-clamp approaches. However, even between single-cell
678 techniques, there are regularly discrepancies and confusing interpretations because cell
679 behaviour is highly sensitive, and often the devil is in the experimental details. Therefore,
680 considerations that will lead to better harmonisation of experimental conditions are
681 timely and relevant, especially regarding the accumulation of large amounts of data in
682 the literature.

683
684

685 **5 Acknowledgements**

686

687 We wish to thank Prof. Water Reinhart and Dr. Thomas Schulzki (Cantonal Hospital
688 Graubünden, Switzerland) for collaboration in data generation for Figure 2B, as well as
689 Dr. Andrea Brüggemann and Dr. Claudia Haarmann (Nanion Technologies GmbH,
690 Munich, Germany) for their assistance with data acquisition for Figure 4. The work was
691 partially funded by the Ministero dell'Università e della Ricerca, Italy, with PRIN2008
692 funds to G.M.

693

694

695 **6 References**

696

- 697 1. Swammerdam J. *Bybel der Natuur*. London: Bookseller C. G. Seyffert; 1737.
- 698 2. Staines HM, Alkhalil A, Allen RJ, et al. Electrophysiological studies of malaria
699 parasite-infected erythrocytes: current status. *Int. J. Parasitol.* 2007;37(5):475–
700 482.
- 701 3. Bouyer G, Egée S, Thomas SLY. Toward a unifying model of malaria-induced
702 channel activity. *Proceedings of the National Academy of Sciences of the United*
703 *States of America.* 2007;104(26):11044–11049.
- 704 4. Salzer U, Prohaska R. Stomatin, flotillin-1, and flotillin-2 are major integral proteins
705 of erythrocyte lipid rafts. *Blood.* 2001;97(4):1141–1143.
- 706 5. Ciana A, Balduini C, Minetti G. Detergent-resistant membranes in human
707 erythrocytes and their connection to the membrane-skeleton. *J. Biosci.*
708 2005;30(3):317–328.
- 709 6. Ciana A, Achilli C, Balduini C, Minetti G. On the association of lipid rafts to the
710 spectrin skeleton in human erythrocytes. *Biochimica et Biophysica Acta.*
711 2011;1808(1):183–190.
- 712 7. Grygorczyk R, Schwarz W, Passow H. Ca²⁺-activated K⁺ channels in human red
713 cells. Comparison of single-channel currents with ion fluxes. *Biophysj.*
714 1984;45(4):693–698.
- 715 8. Brugnara C, de Franceschi L. Ca²⁺-activated K⁺ transport in erythrocytes.
716 Comparison of binding and transport inhibition by scorpion toxins. *Journal of*
717 *Biological Chemistry.* 1993;268(12):8760–8768.
- 718 9. Yang L, Andrews DA, Low PS. Lysophosphatidic acid opens a Ca⁺⁺ channel in
719 human erythrocytes. *Blood.* 2000;95(7):2420–2425.
- 720 10. Kaestner L, Tabellion W, Lipp P, Bernhardt I. Prostaglandin E2 activates channel-

- 721 mediated calcium entry in human erythrocytes: an indication for a blood clot
722 formation supporting process. *Thrombosis and Haemostasis*. 2004;92(6):1269–
723 1272.
- 724 11. Kucherenko YV, Weiss E, Bernhardt I. Effect of the ionic strength and
725 prostaglandin E2 on the free Ca²⁺ concentration and the Ca²⁺ influx in human red
726 blood cells. *Bioelectrochemistry*. 2004;62(2):127–133.
- 727 12. O'Neill JS, Reddy AB. Circadian clocks in human red blood cells. *Nature*.
728 2011;469(7331):498–503.
- 729 13. Beutler E, West C, Blume KG. Removal of Leukocytes and Platelets From Whole-
730 Blood. *Journal of Laboratory and Clinical Medicine*. 1976;88(2):328–333.
- 731 14. Achilli C, Ciana A, Balduini C, Risso A, Minetti G. Application of gelatin
732 zymography for evaluating low levels of contaminating neutrophils in red blood cell
733 samples. *Analytical biochemistry*. 2011;409(2):296–297.
- 734 15. Beutler E, GELBART T. The Mechanism of Removal of Leukocytes by Cellulose
735 Columns. *Blood Cells*. 1986;12(1):57–64.
- 736 16. Rebullà P, Porretti L, Bertolini F, et al. White cell-reduced red cells prepared by
737 filtration: a critical evaluation of current filters and methods for counting residual
738 white cells. *Transfusion*. 1993;33(2):128–133.
- 739 17. Bourne PK, Cossins AR. On the instability of K⁺ influx in erythrocytes of the
740 rainbow trout, *Salmo gairdneri*, and the role of catecholamine hormones in
741 maintaining in vivo influx activity. *The Journal of experimental biology*.
742 1982;101:93–104.
- 743 18. Mihov D, Vogel J, Gassmann M, Bogdanova AY. Erythropoietin activates nitric
744 oxide synthase in murine erythrocytes. *American journal of physiology*.
745 2009;297(2):C378–88.
- 746 19. Sarkadi B, Szasz I, Gerloczy A, Gardos G. Transport Parameters and
747 Stoichiometry of Active Calcium-Ion Extrusion in Intact Human Red-Cells.
748 *Biochimica et Biophysica Acta*. 1977;464(1):93–107.
- 749 20. Canestrari F, Galli F, Boschi S, et al. Erythrocyte Na⁺,K⁽⁺⁾-ATPase properties and
750 adenylate energy charge in normotensives and in essential hypertensives. *Clinica
751 Chimica Acta*. 1994;224(2):167–179.
- 752 21. Ellory JC, Hall AC. Temperature effects on red cell membrane transport
753 processes. *Symposia of the Society for Experimental Biology*. 1987;41:53–66.
- 754 22. Grygorczyk R. Temperature dependence of Ca²⁺-activated K⁺ currents in the
755 membrane of human erythrocytes. *Biochimica et Biophysica Acta*.
756 1987;902(2):159–168.
- 757 23. Li Q, Jungmann V, Kiyatkin A, Low PS. Prostaglandin E2 stimulates a Ca²⁺-
758 dependent K⁺ channel in human erythrocytes and alters cell volume and
759 filterability. *The Journal of biological chemistry*. 1996;271(31):18651–18656.
- 760 24. Kleinbongard P, Schulz R, Rassaf T, et al. Red blood cells express a functional
761 endothelial nitric oxide synthase. *Blood*. 2006;107(7):2943–2951.
- 762 25. Staines HM, Powell T, Ellory JC, et al. Modulation of whole-cell currents in
763 Plasmodium falciparum-infected human red blood cells by holding potential and
764 serum. *J. Physiol. (Lond.)*. 2003;552(Pt 1):177–183.
- 765 26. Glogowska E, Dyrda A, Cuffe A, et al. Anion conductance of the human red cell is

- 766 carried by a maxi-anion channel. *Blood Cells, Molecules, and Diseases*.
767 2010;44(4):243–251.
- 768 27. Duranton C, Tanneur V, Lang C, et al. A High Specificity and Affinity Interaction
769 with Serum Albumin Stimulates an Anion Conductance in Malaria-Infected
770 Erythrocytes. *Cellular Physiology and Biochemistry*. 2008;22(5-6):395–404.
- 771 28. Makhro A, Wang J, Vogel J, et al. Functional NMDA receptors in rat erythrocytes.
772 *AJP: Cell Physiology*. 2010;298(6):C1315–C1325.
- 773 29. Valeri CR, Zaroulis. Rejuvenation and Freezing of Outdated Stored Human Red-
774 Cells. *New Engl J Med*. 1972;287(26):1307–&.
- 775 30. Barshtein G, Manny N, Yedgar S. Circulatory risk in the transfusion of red blood
776 cells with impaired flow properties induced by storage. *Transfus Med Rev*.
777 2011;25(1):24–35.
- 778 31. Lang KS, Lang PA, Bauer C, et al. Mechanisms of suicidal erythrocyte death.
779 *Cellular Physiology and Biochemistry*. 2005;15(5):195–202.
- 780 32. Huber SM, Uhlemann AC, Gamper NL, et al. Plasmodium falciparum activates
781 endogenous Cl(-) channels of human erythrocytes by membrane oxidation. *The*
782 *EMBO Journal*. 2002;21(1-2):22–30.
- 783 33. Huber S, Uhlemann A, Gamper N, et al. Oxidative permeabilization? *Trends in*
784 *Parasitology*. 2002;18(8):346.
- 785 34. Dumaswala UJ, Zhuo L, Jacobsen DW, Jain SK, Sukalski KA. Protein and lipid
786 oxidation of banked human erythrocytes: role of glutathione. *Free Radical Biology*
787 *& Medicine*. 1999;27(9-10):1041–1049.
- 788 35. Lutz H, Bussolino F, Flepp R, Fasler S. Naturally occurring anti-band-3 antibodies
789 and complement activation together mediate phagocytosis of oxidatively stressed
790 human erythrocytes. *Proceedings of the National Academy of Science of the*
791 *United States of America*. 1987;(84):7368–73687372.
- 792 36. Lang KS, Duranton C, Poehlmann H, et al. Cation channels trigger apoptotic death
793 of erythrocytes. *Cell Death and Differentiation*. 2003;10(2):249–256.
- 794 37. Bogdanova A, Mihov D, Lutz H, et al. Enhanced erythro-phagocytosis in
795 polycythemic mice overexpressing erythropoietin. *Blood*. 2007;110(2):762–769.
- 796 38. Huber SM, Gamper N, Lang F. Chloride conductance and volume-regulatory
797 nonselective cation conductance in human red blood cell ghosts. *Pflügers Archiv -*
798 *European Journal of Physiology*. 2001;441(4):551–558.
- 799 39. Huber SM, Duranton C, Henke G, et al. Plasmodium induces swelling-activated
800 ClC-2 anion channels in the host erythrocyte. *The Journal of Biological Chemistry*.
801 2004;279(40):41444–41452.
- 802 40. van Faassen EE, Babrami S, Feelisch M, et al. Nitrite as Regulator of Hypoxic
803 Signaling in Mammalian Physiology. *Medicinal Research Reviews*.
804 2009;29(5):683–741.
- 805 41. Bogdanova A, Berenbrink M, Nikinmaa M. Oxygen-dependent ion transport in
806 erythrocytes. *Acta Physiologica*. 2009;195(3):305–319.
- 807 42. Decherf G, Bouyer G, Egée S, Thomas SLY. Chloride channels in normal and
808 cystic fibrosis human erythrocyte membrane. *Blood Cells, Molecules, and*
809 *Diseases*. 2007;39(1):24–34.
- 810 43. Deplaine G, Safeukui I, Jeddi F, et al. The sensing of poorly deformable red blood

- 811 cells by the human spleen can be mimicked in vitro. *Blood*. 2011;117(8):e88–e95.
- 812 44. Red Blood Cells of Domestic Mammals. Amsterdam, New York: Elsevier Science
813 Ltd; 1983.
- 814 45. Glomski CA, Pica A. The Avian Erythrocyte: Its Phylogenetic Odyssey. Science
815 Publishers, CRC Press; 2011.
- 816 46. Lassen UV, Pape L, Vestergaard-Bogind B, Bengtson O. Calcium-related
817 hyperpolarization of the Amphiuma red cell membrane following micropuncture.
818 *The Journal of Membrane Biology*. 1974;18(2):125–144.
- 819 47. Ellory JC, Tucker EM. Cation transport in red blood cells. *Red Blood Cells of*
820 *Domestic Mammals*. 1983;291–314.
- 821 48. Nguyen DB, Wagner-Britz L, Maia S, et al. Regulation of phosphatidylserine
822 exposure in red blood cells. *Cellular Physiology and Biochemistry*. 2011;28:847–
823 856.
- 824 49. Bernhardt I, Hall AC, Ellory JC. Transport Pathways for Monovalent Cations
825 through Erythrocyte Membranes. 1988;126(1):5–21.
- 826 50. Van Dijck PW, De Kruijff B, Van Deenen LL, De Gier J, Demel RA. The preference
827 of cholesterol for phosphatidylcholine in mixed phosphatidylcholine-
828 phosphatidylethanolamine bilayers. *Biochimica et Biophysica Acta*.
829 1976;455(2):576–587.
- 830 51. Saito M, Tanaka Y, Ando S. Thin-layer chromatography-densitometry of minor
831 acidic phospholipids: application to lipids from erythrocytes, liver, and kidney.
832 *Anal. Biochem*. 1983;132(2):376–383.
- 833 52. Dovichi NJ, Hu S, Michels D, Mao D, Dambrowitz A. Single Cell Proteomics.
834 *Single Cell Analysis: Technologies and Applications*. 2009;(4):69–90.
- 835 53. Pasini EM, Kirkegaard M, Mortensen P, et al. In-depth analysis of the membrane
836 and cytosolic proteome of red blood cells. *Blood*. 2006;108(3):791–801.
- 837 54. Gusev GP, Fleishman DG, Nikiforov VA, Sherstobitov AO. Potassium channels of
838 the lamprey erythrocyte membrane exhibit a high selectivity to K⁺ over Rb⁺: a
839 comparative study of 86Rb and 41K transport. *General physiology and biophysics*.
840 1997;16(3):273–284.
- 841 55. Cavieres JD, Ellory JC. The interaction of monovalent cations with the sodium
842 pump of low-potassium goat erythrocytes. *J. Physiol. (Lond.)*. 1977;271:289–318.
- 843 56. Lew VL, Hockaday A, Sepulveda MI, et al. Compartmentalization of Sickle-Cell
844 Calcium in Endocytic Inside-Out Vesicles. *Nature*. 1985;315(6020):586–589.
- 845 57. Rhoda MD, Giraud F, Craescu CT, Beuzard Y. Compartmentalization of Ca²⁺ in
846 sickle cells. *Cell Calcium*. 1985;6(5):397–411.
- 847 58. Hamill OP. Potassium and Chloride Channels in Red Blood Cells. *Single Channel*
848 *Recording*. 1983;451–471.
- 849 59. Desai S, Bezrukov S, Zimmerberg J. A voltage-dependent channel involved in
850 nutrient uptake by red blood cells infected with the malaria parasite. *Nature*.
851 2000;406(6799):1001–1005.
- 852 60. Christophersen P, Bennekou P. Evidence for a voltage-gated, non-selective cation
853 channel in the human red cell membrane. *Biochimica et Biophysica Acta*.
854 1991;1065(1):103–106.
- 855 61. Kaestner L, Bollensdorff C, Bernhardt I. Non-selective voltage-activated cation

- 856 channel in the human red blood cell membrane. *Biochimica et Biophysica Acta*.
857 1999;1417(1):9–15.
- 858 62. Egée S, Lapaix F, Decherf G, et al. A stretch-activated anion channel is up-
859 regulated by the malaria parasite *Plasmodium falciparum*. *J. Physiol. (Lond.)*.
860 2002;542(Pt 3):795–801.
- 861 63. Duranton C, Huber SM, Lang F. Oxidation induces a Cl(-)-dependent cation
862 conductance in human red blood cells. *J. Physiol. (Lond.)*. 2002;539(Pt 3):847–
863 855.
- 864 64. Bouyer G, Cueff A, Egée S, et al. Erythrocyte peripheral type benzodiazepine
865 receptor/voltage-dependent anion channels are upregulated by *Plasmodium*
866 *falciparum*. *Blood*. 2011;118(8):2305–2312.
- 867 65. Thomas SLY, Bouyer G, Cueff A, et al. Ion channels in human red blood cell
868 membrane: Actors or relics? *Blood Cells, Molecules, and Diseases*. 2011;46:261–
869 265.
- 870 66. Hamill OP. Potassium channel currents in human red blood cells. *The Journal of*
871 *physiology*. 1981;319:97P–98P.
- 872 67. Kaestner L, Bernhardt I. Ion channels in the human red blood cell membrane: their
873 further investigation and physiological relevance. *Bioelectrochemistry*. 2002;55(1-
874 2):71–74.
- 875 68. Huber SM, Duranton C, Lang F. Patch-clamp analysis of the “new permeability
876 pathways” in malaria-infected erythrocytes. *International Review of Cytology*.
877 2005;246:59–134.
- 878 69. Browning JA, Staines HM, Robinson HC, et al. The effect of deoxygenation on
879 whole-cell conductance of red blood cells from healthy individuals and patients
880 with sickle cell disease. *Blood*. 2007;109(6):2622–2629.
- 881 70. Johnson RM. Membrane Stress Increases Cation Permeability in Red Cells.
882 *Biophysical Journal*. 1994;67(5):1876–1881.
- 883 71. Dyrda A, Cytlak U, Ciuraszkiewicz A, et al. Local membrane deformations activate
884 Ca²⁺-dependent K⁺ and anionic currents in intact human red blood cells. *PLoS*
885 *ONE*. 2010;5(2):e9447.
- 886 72. Hoffman JF, Kaplan JH, Callahan TJ, Freedman JC. Electrical resistance of the
887 red cell membrane and the relation between net anion transport and the anion
888 exchange mechanism. *Annals of the New York Academy of Sciences*.
889 1980;341:357–360.
- 890 73. Red Cell Membrane Transport in Health and Disease. 2003;139–152.
- 891 74. Fettiplace R, Andrews D. The Thickness, Composition and Structure of Some
892 Lipid Bilayers and Natural Membranes. *Journal of Membrane Biology*. 1971.
- 893 75. Rodighiero S, De Simoni A, Formenti A. The voltage-dependent nonselective
894 cation current in human red blood cells studied by means of whole-cell and
895 nystatin-perforated patch-clamp techniques. *Biochimica et Biophysica Acta*.
896 2004;1660(1-2):164–170.
- 897 76. Lew VL, Bookchin RM. Ion transport pathology in the mechanism of sickle cell
898 dehydration. *Physiological Reviews*. 2005;85(1):179–200.
- 899 77. Lew VL, Etzion Z, Bookchin RM. Dehydration response of sickle cells to sickling-
900 induced Ca(++) permeabilization. *Blood*. 2002;99(7):2578–2585.

- 901 78. Staines HM, Ashmore S, Felgate H, et al. Solute transport via the new
902 permeability pathways in Plasmodium falciparum-infected human red blood cells is
903 not consistent with a simple single-channel model. *Blood*. 2006;108(9):3187–
904 3194.
- 905 79. Larsen FL, Katz S, Roufogalis BD, Brooks DE. Physiological shear stresses
906 enhance the Ca²⁺ permeability of human erythrocytes. *Nature*.
907 1981;294(5842):667–668.
- 908 80. Suh TK, Schenk JL, Seidel GE. High pressure flow cytometric sorting damages
909 sperm. *Theriogenology*. 2005;64(5):1035–1048.
- 910 81. Kaestner L, Lipp P. Towards Imaging the Dynamics of Protein Signalling. *Imaging*
911 *Cellular and Molecular Biological Functions*. 2007;289–312.
- 912 82. Kaestner L. Cation Channels in Erythrocytes - Historical and Future Perspective.
913 *The Open Biology Journal*. 2011;4:27–34.
- 914 83. Komorowska M, Cuissot A, Czarnoński A, Białas W. Erythrocyte response to
915 near-infrared radiation. *Journal of Photochemistry and Photobiology B: Biology*.
916 2002;68(2-3):93–100.
- 917 84. Kaestner L, Juzeniene A, Moan J. Erythrocytes-the “house elves” of photodynamic
918 therapy. *Photochem. Photobiol. Sci.* 2004;3(11-12):981–989.
- 919 85. Förster T. Intermolecular energy migration and fluorescence. *Annals of Physics*.
920 1948;6:.
- 921 86. Esposito A, Tiffert T, Mauritz JMA, et al. FRET imaging of hemoglobin
922 concentration in Plasmodium falciparum-infected red cells. *PLoS ONE*.
923 2008;3(11):e3780.
- 924 87. Chien S, Jan K-M. Ultrastructural Basis of the Mechanism of Rouleaux Formation.
925 *Microvascular Research*. 1973;5:155–166.
- 926 88. Rampling MW, Whittingstall P. A comparison of five methods for estimating red
927 cell aggregation. *Klinische Wochenschrift*. 1986;64(20):1084–1088.
- 928 89. Baskurt O, Neu B, Meiselman HJ. Red blood Cell Aggregation. Boca Raton: CRC
929 Press; 2012.
- 930 90. Picart C, Piau JM, Galliard H, Carpentier P. Human blood shear yield stress and
931 its hematocrit dependence. *Journal of Rheology*. 1998;42(1):1–12.
- 932 91. Shin S, Park M, Jang J, Ku Y, Suh J. Measurement of red blood cell aggregation
933 by analysis of light transmission in a pressure-driven slit flow system. *Korea-*
934 *Australia Rheology Journal*. 2004;16(3):129–134.
- 935 92. Steffen P, Jung A, Nguyen DB, et al. Stimulation of human red blood cells leads to
936 Ca²⁺-mediated intercellular adhesion. *Cell Calcium*. 2011;50:54–61.
- 937 93. Kaestner L, Steffen P, Nguyen DB, et al. Lysophosphatidic acid induced red blood
938 cell aggregation in vitro. *Bioelectrochemistry*. 2011.
- 939 94. Carvalho FA, de Oliveira S, Freitas T, Gonçalves S, Santos NC. Variations on
940 fibrinogen-erythrocyte interactions during cell aging. *PLoS ONE*.
941 2011;6(3):e18167.
- 942 95. Minetti G, Ciana A, Profumo A, et al. Cell age-related monovalent cations content
943 and density changes in stored human erythrocytes. *Biochimica et Biophysica Acta*.
944 2001;1527(3):149–155.
- 945 96. Dodge JT, Mitchell C, Hanahan DJ. The preparation and chemical characteristics

- 946 of hemoglobin-free ghosts of human erythrocytes. *Archives of biochemistry and*
947 *biophysics*. 1963;100(1):119–130.
- 948 97. Barry PH, Lynch JW. Liquid junction potentials and small cell effects in patch-
949 clamp analysis. *The Journal of Membrane Biology*. 1991;121(2):101–117.
- 950 98. Cahalan MD, Chandy KG, DeCoursey TE, Gupta S. A voltage-gated potassium
951 channel in human T lymphocytes. *J. Physiol. (Lond.)*. 1985;358(1):197–237.
- 952 99. Kaestner L. Calcium signalling: Approaches and Findings in the Heart and Blood.
953 Heidelberg: Springer Verlag; 2012.

954
955

956 **Figure legends**

957

958 **Figure 1:** (A) Gelatin zymography of the pelleted cell fraction obtained by the
959 “Accuspin™ System-Histopaque®-1077” method (Sigma-Aldrich, Inc., St. Louis, MO,
960 USA) used in a recent work for isolating RBCs in supposedly pure form¹². As per the
961 manufacturer’s instructions, a blood sample was freshly drawn in 0.1 volumes of 3.8%
962 (w/v) tri-sodium citrate as the anticoagulant and immediately layered in the Accuspin™
963 tube. After centrifugation, the RBC pellet was collected (after removal of the septum from
964 the Accuspin™ tube), washed two times in ten volumes of PBS and processed for
965 gelatin zymography, as previously described¹⁴. The arrows indicate the bands
966 corresponding to the typical pattern of in-gel digestion of gelatin by the granulocytic pro-
967 metalloproteinase 9 and its higher molecular weight aggregate with lipocalin and are
968 indicative of the presence of PMNs in the RBC fractions. The lane marked “T”
969 corresponds to unseparated blood cells. The lane marked “F” contains a sample of
970 RBCs that was passed through a cellulose filter to remove leukocytes and platelets and
971 is indeed free of PMNs. The pellet of supposedly pure RBCs resulting from the
972 Accuspin™ separation contains almost all of the PMNs that were present in the
973 unseparated blood (“AH”). The lane marked “H” is a sample of RBCs obtained by
974 density centrifugation in the Histopaque®-1077 solution but in a standard tube (not
975 Accuspin™). In each lane, the equivalent of 10^7 cells was loaded. In the lane “PMNs”,
976 2×10^2 pure PMNs were loaded. (B) Contaminating PMNs are carried all along during the
977 preparation of ghost membranes, and they ended up in the final sample of supposedly
978 pure ghosts. PMNs were detected using gelatin zymography¹⁴ in ghosts prepared from
979 washed (“W”) or filtered (“F”) RBCs with the method of Dodge⁹⁶ as previously detailed⁵,
980 but with the omission of phenyl-methyl-sulphonyl-fluoride to show the consequences of
981 proteolysis. Where proteolysis was inhibited, diisopropylfluorophosphate (DFP) was
982 used at a final concentration of 1 mM in PBS, to pre-treat RBCs for 5 min at 25 °C before
983 hypotonic haemolysis to prepare the ghosts. During ghost preparation, at the end of the
984 third sedimentation, the “button” of dark, thick material that forms at the bottom of the
985 ghosts and that is especially visible in samples where contamination by PMNs is high
986 was either removed or left in place (“button” - or +). After preparation, the ghost
987 suspension was brought to the volume of the original packed RBCs and processed for
988 gelatin zymography as described¹⁴. In each lane, the equivalent of 10^7 RBCs was loaded.
989 Pure PMNs were loaded as a standard in the adjacent lanes, in the numbers given. (C)
990 The ghosts prepared in the various modes described above were processed for SDS-

991 PAGE and Western blotting. Analysis of ankyrin and protein 4.1 revealed that both
992 proteins were quantitatively decreased when the ghosts were prepared from filtered or
993 washed RBCs in the absence of DFP. When the “button” of debris was not removed,
994 both proteins were heavily damaged.

995
996 **Figure 2: (A)** Changes in morphology and in the intracellular Ca^{2+} levels in RBCs from a
997 sickle cell patient caused by inhibition of the Ca^{2+} pump. RBCs from a sickle cell disease
998 patient suspended in isotonic medium containing 1.8 mM CaCl_2 , 10 mM glucose and
999 0.1% bovine serum albumin. The cells were loaded with 10 μM Fluo-4 AM for 40 min in
1000 the presence or absence of 5 mM Na-orthovanadate (ov). The upper panels show bright
1001 field images of control and orthovanadate-treated cells, and the lower panels represent
1002 the corresponding readouts of Fluo-4 fluorescence. Extensive vesiculation, cell
1003 disintegration and echinocytosis followed uncontrolled Ca^{2+} loading. **(B)** RBCs from two
1004 healthy subjects (P1 and P2) were collected, filtered and stored for 1-21 days in Ca^{2+} -
1005 free citrate-containing glutathione (GSH) conservation solution, and they were then re-
1006 suspended in the incubation medium containing 145 mM NaCl, 4 mM KCl, 1.8 mM Ca^{2+} ,
1007 10 mM glucose and 0.1% bovine serum albumin. The cells of both donors retained
1008 normal discocyte morphology over at least one week in the citrate phosphate dextrose
1009 solution, and P1 was considered "a better quality donor" during conventional quality
1010 control tests. Of importance are the inter-individual differences in the responses and
1011 acute changes in morphology in the presence of extracellular Ca^{2+} and the progressive
1012 deterioration of cellular quality associated with ATP and GSH depletion and changes in
1013 the ion and water content.

1014
1015 **Figure 3:** Electrical model of a patch-clamp for cell-attached **(A)** and whole-cell **(B)**
1016 configurations. **(A)** When narrowing the tip of the pipette, its resistance R_{pip} is increased.
1017 Adaptation of the shape of the pipettes for RBCs (especially human RBCs) has led to
1018 the use of pipettes with an R_{pip} between 10 and 15 M Ω . Up to 80% of seal attempts are
1019 successful with such pipettes, depending on the solutions used. These values are not a
1020 problem for single channel studies, as they remain well below the patch resistance R_{patch}
1021 through which single channel currents are recorded and these currents can therefore be
1022 easily recorded. However, as suggested by Barry and Lynch, distortion of the potential
1023 that is applied to the membrane can occur in small cells in relation to the global
1024 membrane resistance of the cell R_m ⁹⁷. This resistance in small cells can be on the order
1025 of magnitude of several G Ω , which is not much lower than R_{patch} . Then, variations in the
1026 pipette potential can induce changes in the global membrane potential, and this would
1027 result in large errors in the estimation of the single-channel conductance and of the
1028 reversal potential. Barry and Lynch⁹⁷ conclude their work by revealing the distortion
1029 between the apparent and real conductance of the single channel conductance:
1030 $\gamma_c = \gamma_{\text{app}}(1 + R_m/R_{\text{patch}})$, where γ_c and γ_{app} are the real and apparent conductance of the
1031 channel, respectively. This clearly highlights the possible distortion of conductance
1032 estimation with cells showing a high membrane resistance. **(B)** For whole-cell
1033 experiments, two resistances are used in parallel in the electrical model: the global
1034 membrane resistance R_m and the seal resistance R_{seal} . The complexity when using this
1035 configuration with small cells is linked to the possibly high value of membrane resistance.

1036 The seal resistance is barely higher than 100 G Ω , and in small cells, such as RBCs, the
1037 global resistance can reach this order of magnitude⁹⁸. Then, the contribution of the seal
1038 leak to the currents recorded in this configuration is not negligible: the current measured
1039 between the two electrodes can be attributed either to the membrane current or a seal
1040 leak, and the voltage applied to the pipette might be different from the voltage that
1041 actually occurs at the membrane level. This can induce an underestimation of the
1042 channel conductance and a discrepancy between the real and apparent reversal
1043 potentials in cell-attached experiments as well as an incorrect global conductance and a
1044 shift in the I/V curves in whole-cell experiments.

1045
1046 **Figure 4:** Heterogeneity of RBCs - measurements derived from automated patch-clamp
1047 whole cell recordings (NPC-16 Patchliner, Nanion, Munich, Germany). **(A)** depicts the
1048 voltage protocol. The bath solution contained 80 mM NaCl, 3 mM KCl, 10 mM MgCl₂, 35
1049 mM CaCl₂, and 10 mM HEPES /NaOH, pH 7.4, while the pipette solution contained 50
1050 mM CsCl, 10 mM NaCl, 60 mM CsF, 20 mM EGTA, 10 mM HEPES /CsOH, pH 7.2. The
1051 seal resistance was in the range of 1-5 G Ω at a holding potential of -40 mV. **(B)**
1052 exemplifies the recordings from single RBCs of 2 healthy subjects, (a) and (b). The
1053 current traces are superpositions of leak currents and channel-mediated currents. The
1054 non-Ohmic appearance of the currents indicates to differences in the cellular properties
1055 rather than in the patch resistance. Panel **(C)** shows the I/V plots for the whole cell
1056 currents (mean \pm SD, n=24 cells per subject). Please note that both samples were from
1057 freshly drawn RBCs (experiments within 2 h) and are not attributed to different cell
1058 treatments as outlined in Figure 2.

1059
1060 **Figure 5:** Fluorescence spectra of the Ca²⁺ fluorophores Indo-1 and Fluo-4 as well as the
1061 excitation spectra of Fura-2. The normalised fluorescence intensity is plotted against the
1062 wavelength and the Ca²⁺ concentration. For each dye (rows), the spectra were measured
1063 without haemoglobin, with 0.034 g/dl and with 0.34 g/dl haemoglobin (columns). The
1064 arrow points to the heavy spectral alteration of the Indo-1 spectrum in the presence of
1065 0.034 g/dl haemoglobin. Additionally, the Fura-2 spectrum is altered in a way that does
1066 not allow a valid ratiometric read-out. Fluo-4 fluorescence is suppressed, but it seems to
1067 be the best choice for measurements in RBCs due to its high dynamic range⁹⁹. This
1068 figure is a reprint from the original publication Kaestner et al. 2004{Kaestner:2005he}.

1069
1070 **Figure 6:** Panel **(A)** shows a sketch of the working principle of single-cell force
1071 spectroscopy (SCFS). A cell is bound to a cantilever and is brought into contact with
1072 another cell at the surface. During the approach and withdrawal of the cell, the deflection
1073 is monitored and gives direct information about the adhesion force between the cells.
1074 Panel **(B)** shows a sketch of the working principle of the optical tweezers measurements.
1075 Two RBCs are trapped in the foci of two laser beams and are brought into contact. By
1076 measuring the deflection of the cells out of the centre of the laser foci, one can
1077 determine the adhesion force between the cells. Panel **(C)** shows a force vs. distance
1078 curve derived from the SSFS measurements. A weak interaction of approximately 20 pN
1079 can be observed that is only due to an artefact of the measurement (see text). This 20
1080 pN is the lower limit that one can measure using this type of cell with this technique.

1081 Panel (**D**) shows a force calibration of one RBC in an optical trap. It can be observed
1082 that with the given laser power, the trap is only linear up to forces of 15 pN, i.e., this is
1083 the upper limit that can be measured with this technique on these types of cells. Panel
1084 (**A**) is a reprint of the original publication by Steffen et al. 2011⁹², and panels (**B**) and (**D**)
1085 are reprints from the original publication by Kaestner et al. 2011⁹³.

Figure 1

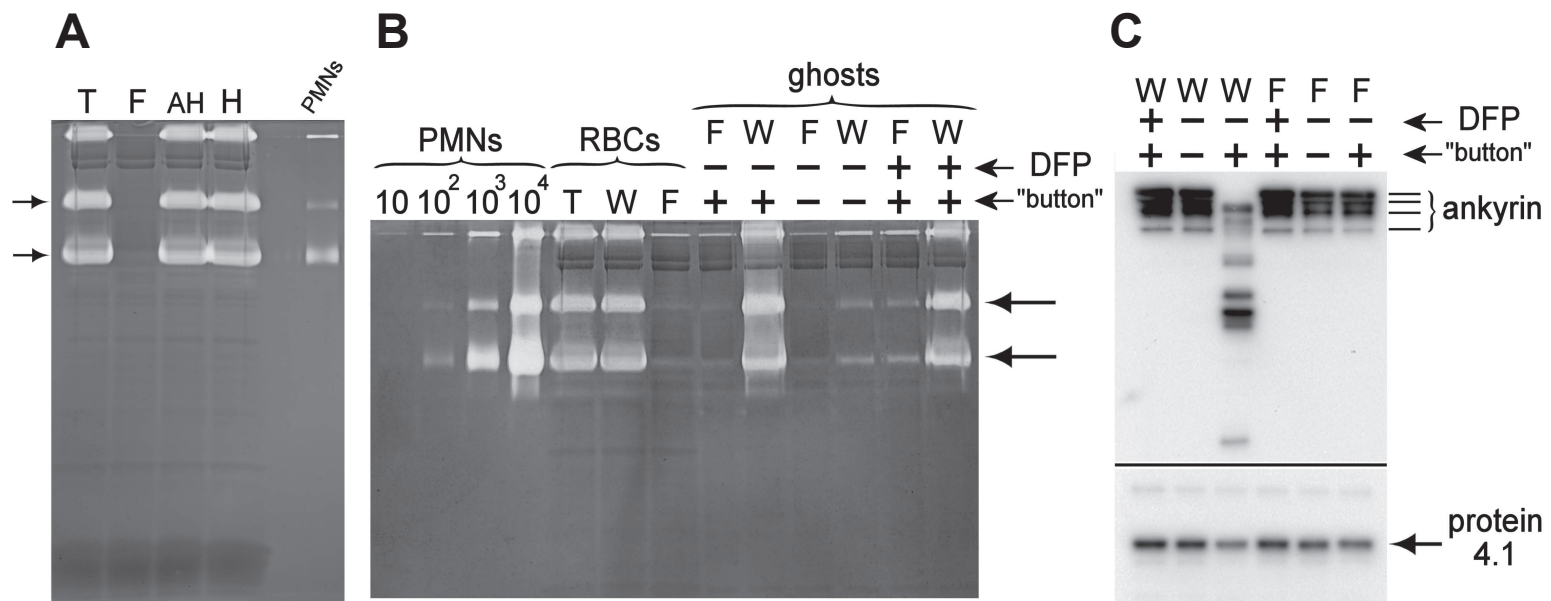


Figure 2

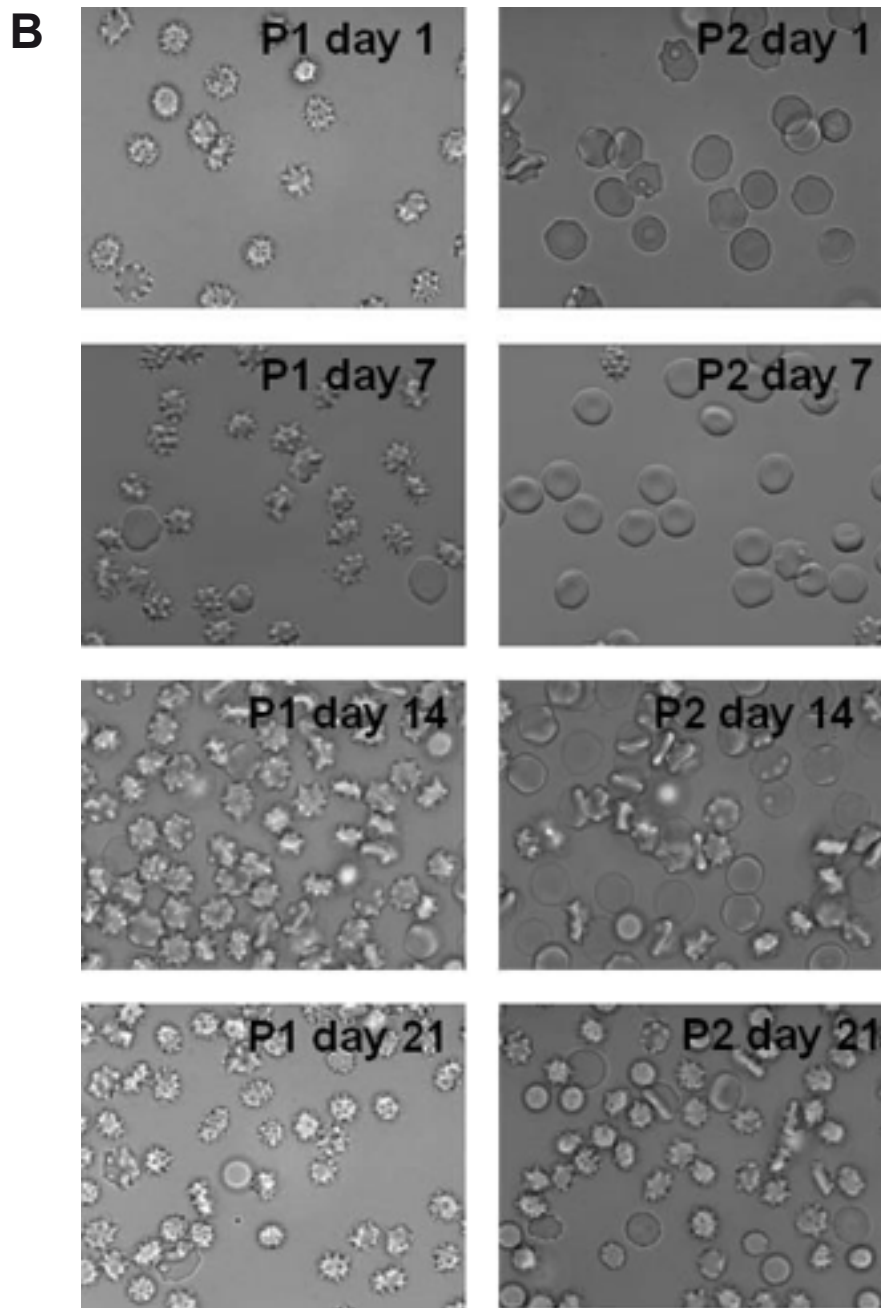
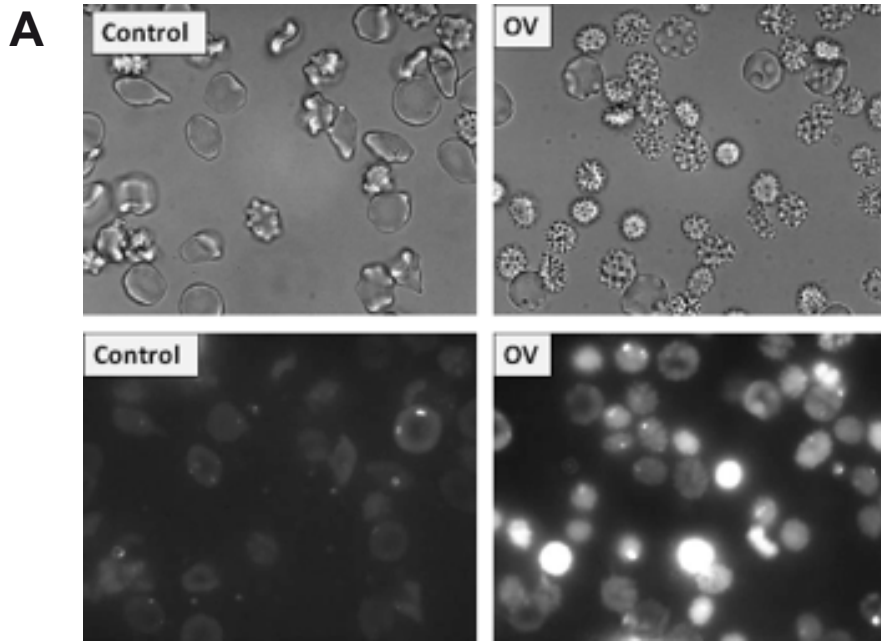
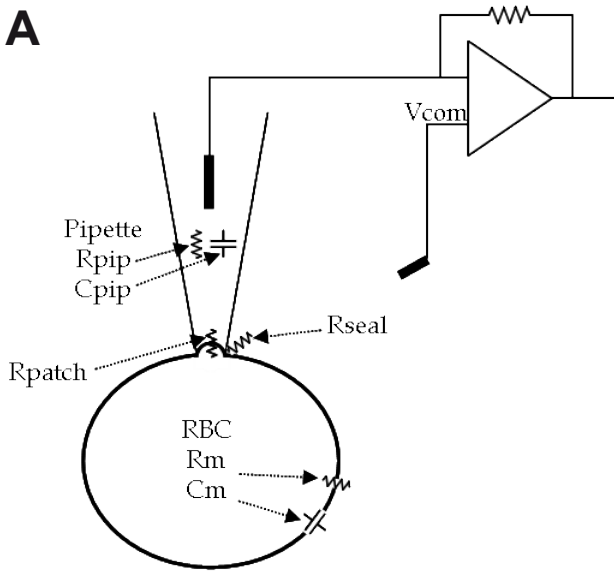


Figure 3

A



B

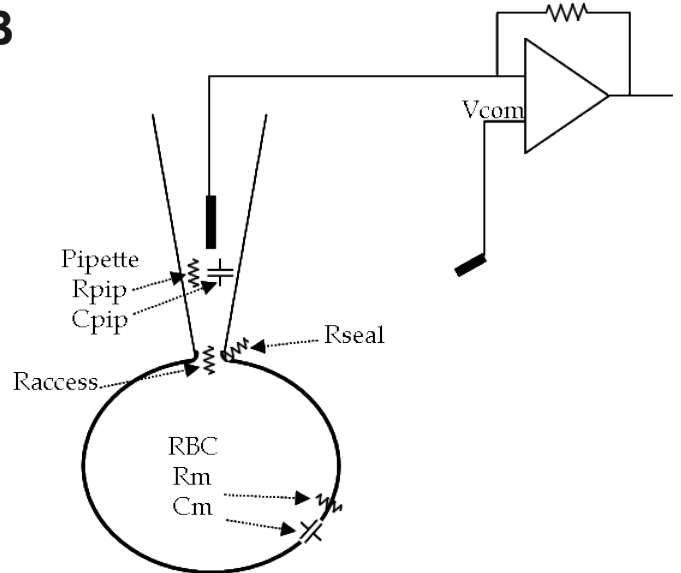


Figure 4

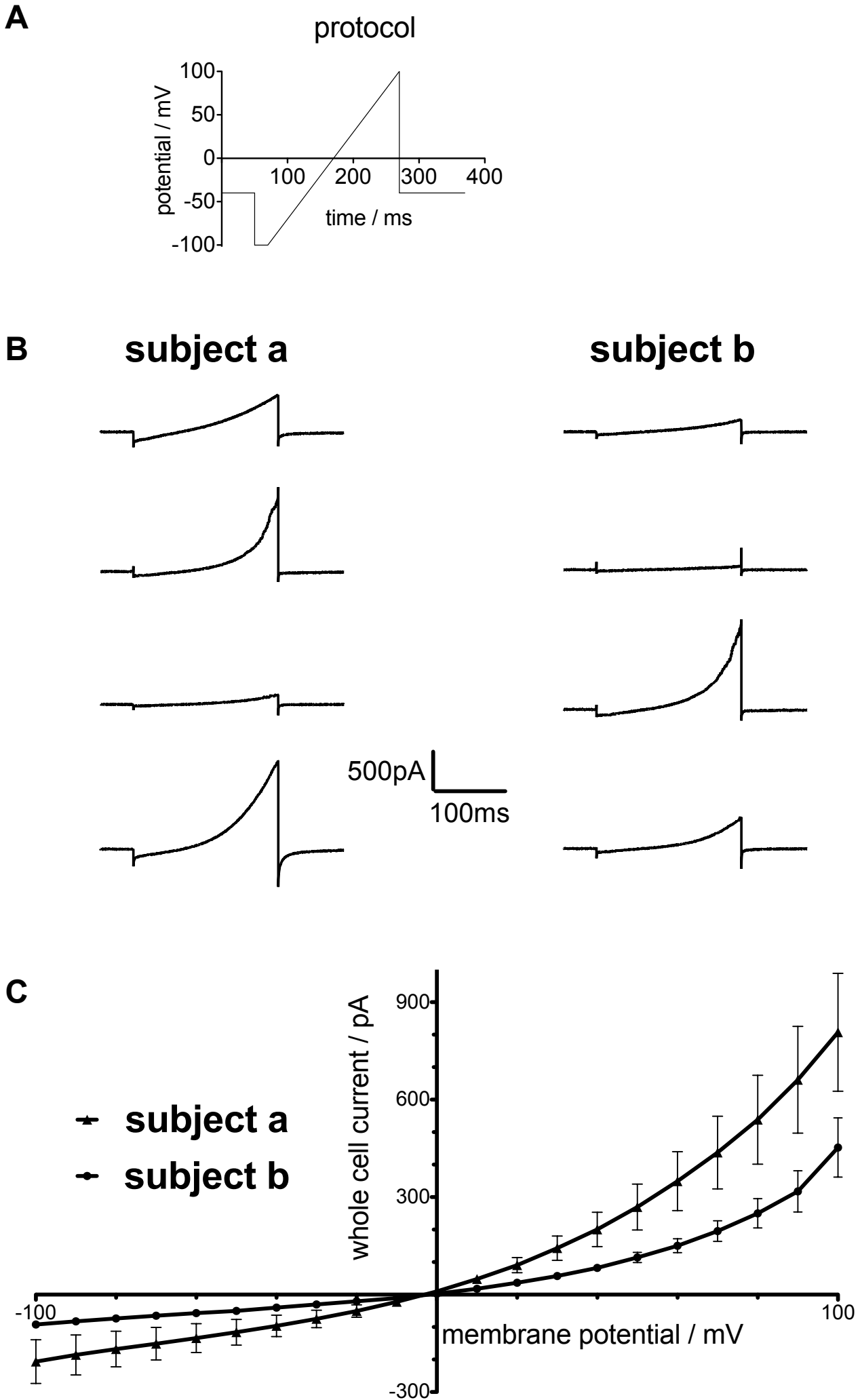


Figure 5

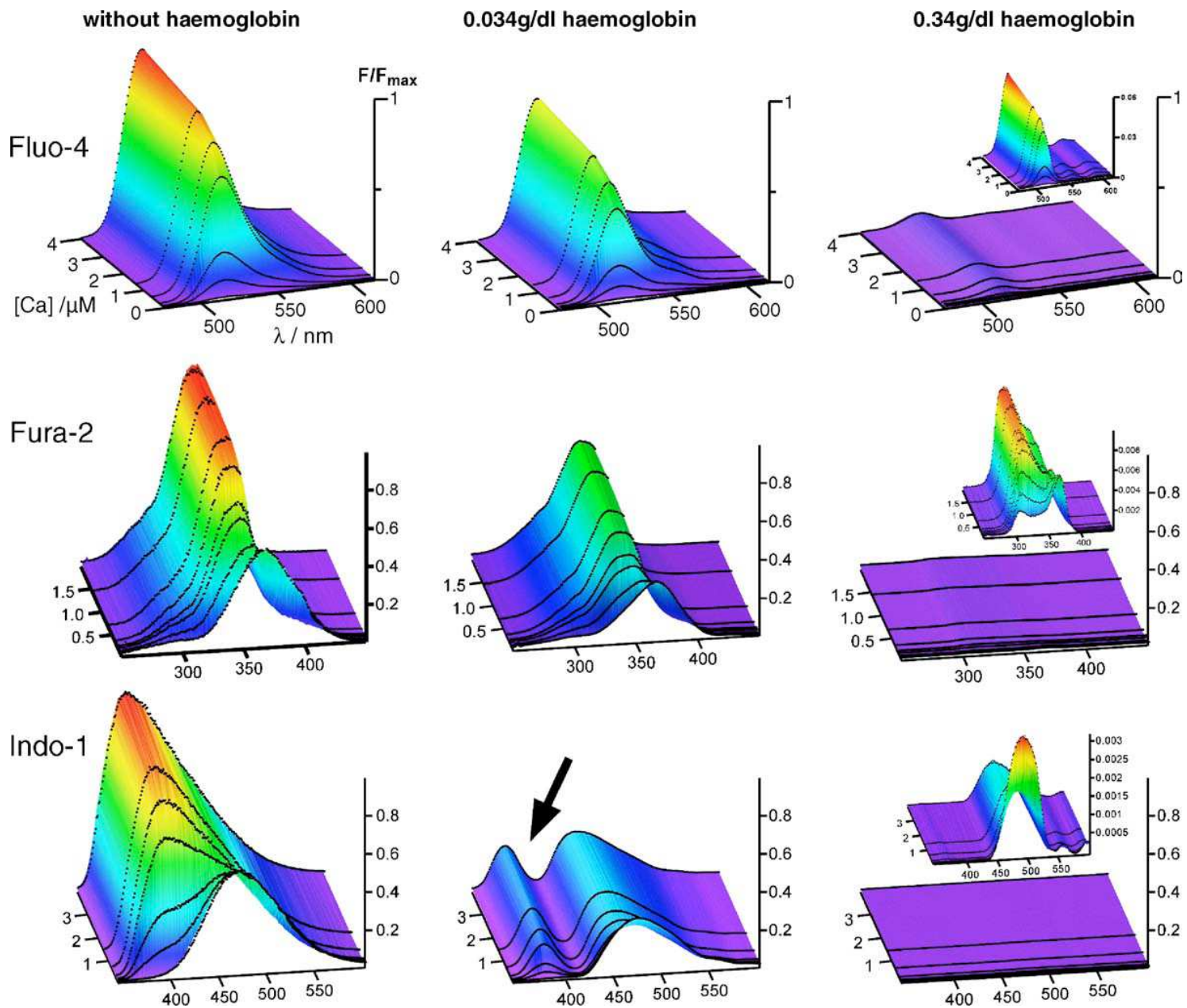
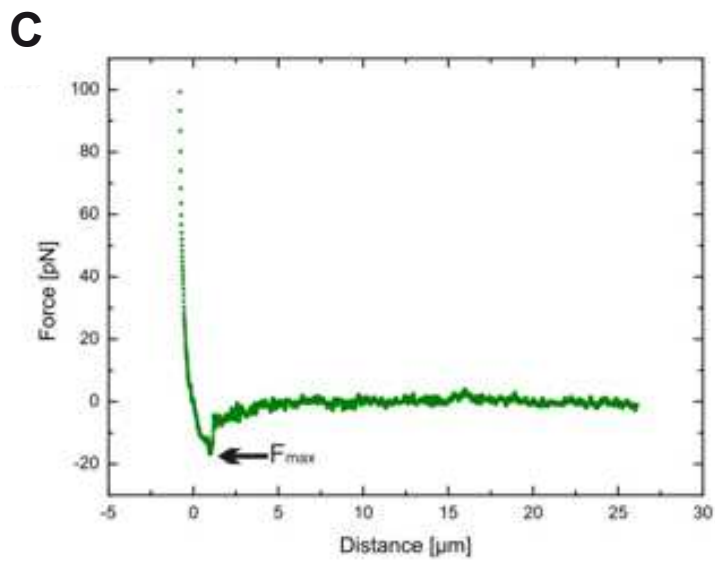
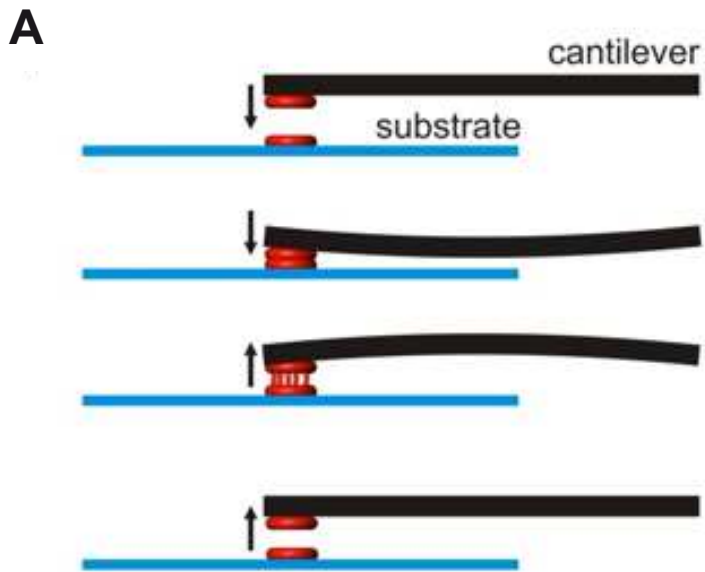
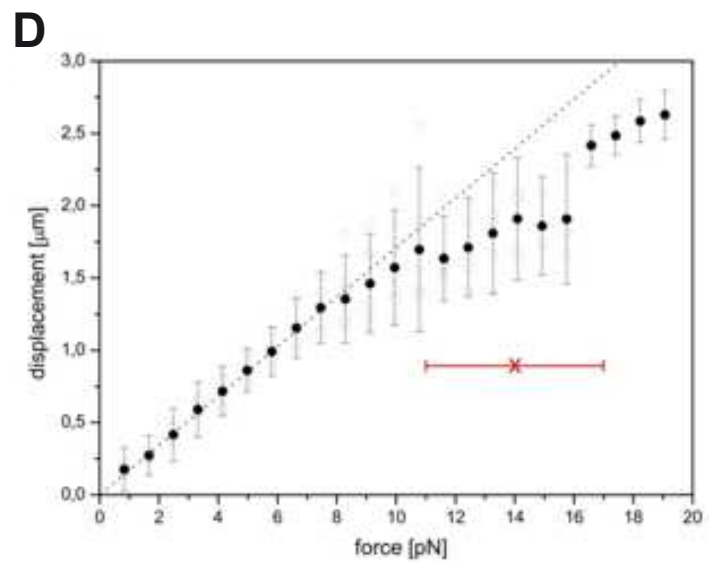


Figure 6



lower limit due to setpoint
pressure of cantilever



upper limit due to cell damage
with increasing laser power